ЖЭТФ, 2014, том 145, вып. 6, стр. 1072–1077

AB INITIO STUDY OF HETEROJUNCTION DISCONTINUITIES IN THE ZnO/Cu_2O SYSTEM

M. Zemzemi [a]*, ***S. Alaya*** [a,b], ***Z. Ben Ayadi*** [a]

[a] *Laboratory of Physics of Materials and Nanomaterials applied at Environment, Faculty of Sciences in Gabes, Gabes University, Erriadh City, Zrig 6072, Gabes, Tunisia*

[b] *King Faisal University, College of Science, Physics Department 31982, Hofuf, Saudi Arabia*

Received October 1, 2013

Solar cells based on transparent conductive oxides such as ZnO/Cu_2O constitute a very advanced way to build high-performance cells. In this work, we are interested in the characterization of the interface through nanoscale modeling based on *ab initio* approaches (density functional theory, local density approximation, and pseudopotential). This work aims to build a supercell containing a heterojunction ZnO/Cu_2O and study the structural properties and the discontinuity of the valence band (band offset) from a semiconducting to another phase. We build a zinc oxide in the wurtzite structure along [0001] on which we place the copper oxide in the hexagonal structure (CdI_2-type). We choose the method of Van de Walle and Martin to calculate the energy offset. This approach fits well with the density functional theory. Our calculation of the band offset gives a value that corresponds to other experimental and theoretical values.

DOI: 10.7868/S0044451014060111

1. INTRODUCTION

Research on photovoltaic energy conversion has recently received great interest [1, 2], and design, growth, and characterization of new-generation solar cells are currently an important research field [3, 4]. In recent years, a large amount of experimental and theoretical work appeared that was focused on heterostructures composed of ultrathin layers designed for new solar energy converters working under a low light intensity. However, the development of new solar cells with improved performances and lower cost requires new approaches based on the use of clean, low cost, and nontoxic materials prepared via low-energy processes. A photovoltaic cell requires two (n-type and p-type) semiconductors.

Zinc oxide (ZnO) attracted the attention of researchers for a long time, owing to its potential applications in many scientific and industrial areas [5]. Actually, its nontoxicity and natural abundance make it an ideal candidate for many industrial manufacturing processes [6]. ZnO belongs to the family of transparent conductive oxides. It is an n-type semiconductor, with a wide band gap of 3.4 eV and an exciton binding energy of 60 meV. These features make ZnO, like GaN, a candidate for applications to blue and ultraviolet optical devices [7].

Cuprous oxide (Cu_2O) is a potential material for the fabrication of low-cost solar cells [8, 9]. The first Cu_2O-based solar cell was manufactured in the late 1920s. However, at that time, and until the first space explorations, the energy production from sun light by the photovoltaic effect was just a curiosity. Cu_2O is a p-type semiconductor with a direct band gap of about 2 eV, which is suitable for photovoltaic conversion.

The ZnO/Cu_2O heterojunction has been synthesized a long time ago and studied for a long time [10]. This heterojunction has recently attracted a renewed interest thanks to the low cost and nontoxic character of its constituents [11–14]. Its efficiency is still quite small (2 %), but better performances can be expected by improving the crystalline order and the interface features. ZnO has a hexagonal (wurtzite) structure, while Cu_2O is cubic (cuprite). An epitaxial growth of (111)-oriented Cu_2O film on the (0001) surface of ZnO is thus possible, as was reported in several pa-

*E-mail: mzemzemi@gmail.com, Mabrouk.Zemzemi@issatgf.rnu.tn

pers [15, 16]. Nevertheless, studies of Cu_2O under pressure show that this crystal undergoes a transition to the hexagonal phase, which is a polytype of the CdI_2 structure [17–19]. This suggests that the growth of Cu_2O films according to the CdI_2 structure on a ZnO substrate is also possible. This kind of growth would have the advantage of giving superlattices preserving the stoichiometry.

In this paper, we investigate this kind of growth. Most of the heterojunction physics is determined by the band offset, which is usually described by models [20–22]. The one by Van de Valle and Martin [23] is used here; combined with *ab initio* calculations, it allow us to calculate the band offset of the ZnO/Cu_2O heterojunction. Previous experimental studies of this heterojunction can be found in Refs. [18, 24], while theoretical results are reported in Ref. [16].

2. COMPUTATIONAL DETAILS

2.1. Density functional theory

The calculations have been performed in the framework of the density functional theory (DFT) [25, 26], using pseudopotentials and a plane-wave basis set as implemented in the Abinit code [27]. Abinit, which is available under a free software licence, allows computing a large set of useful properties of solid-state systems [28]. The valence electron wave functions are expanded in a plane-wave basis set with a kinetic energy cutoff $E_{cut} = 50$ Ha. Troullier–Martins pseudopotentials [29] have been generated by mean of the Fritz-Haber-Institute package [30], for the reference $3d^{10}4s^2$, $3d^{10}4s^1$, and $2s^22p^4$ atomic configurations of zinc, copper, and oxygen, respectively. The exchange-correlation energy and potential are taken into account at the local density approximation (LDA) level by means of the Perdew–Wang [31] parameterization of the quantum Ceperley and Alder Monte Carlo results for a homogeneous electron gas [32]. A (shifted) $8 \times 8 \times 2$ k-point Monkhorst–Pack grid [33] is used for the Brillouin zone sampling.

2.2. Average potential method

The model of Van de Walle and Martin [23] is most widely used for estimating band offsets at semiconductor–semiconductor interfaces. This approach was found to be successful for a variety of materials with nonpolar interfaces. This model can be easily combined with DFT calculations, because the band offset can be deduced from the average self-consistent potential

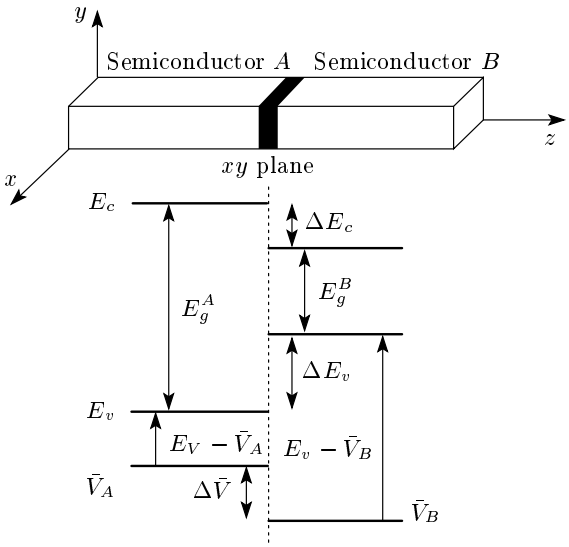

Fig. 1. Schematic diagram of the band alignment of conduction and valence band offsets in a semiconductor heterojunction. The band offsets ΔE_c and ΔE_v are discontinuities in the band at the heterojunction interface

in the superlattice. The success of this simple model reflects the fact that the principal conclusion of the first-principle calculations is that the offsets are essentially intrinsic [34]. To visualize the electrostatic potential profiles extending throughout the heterostructures, $V(x, y, z)$, is averaged over the plane perpendicular to the axis (the xy plane) using the equation

$$\overline{V}(z) = \frac{1}{S} \iint V(x, y, z)\, dx\, dy, \tag{1}$$

where S is the area of a unit cell in the xy plane (Fig. 1). The macroscopic average $\overline{\overline{V}}(z)$ is accomplished by averaging $\overline{V}(z)$ at each point over a distance corresponding to one period a:

$$\overline{\overline{V}}(z) = \frac{1}{a} \int\limits_{z-a/2}^{z+a/2} \overline{V}(z')\, dz', \tag{2}$$

where a is the length of one period in the direction perpendicular to the interface. The macroscopic average potential shows a discontinuity at the interface, indicating that electrons should overcome a potential barrier to cross from the ZnO section to the Cu_2O section. This value is given by

$$\Delta V = \left[\overline{\overline{V}}_{\mathrm{ZnO}} - \overline{\overline{V}}_{\mathrm{Cu_2O}}\right]_{\mathrm{ZnO/Cu_2O}}. \tag{3}$$

The band offset can be determined by aligning the average electrostatic potential across the interface be-

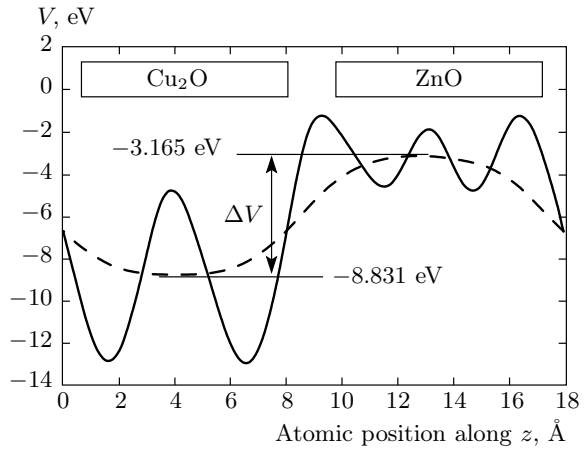

Fig. 2. Variation of the plane and macroscopic average potential for ZnO/Cu_2O in the z direction; ΔV is the potential difference between the macroscopic average potential (dashed line) of ZnO and Cu_2O; the solid line shows the plane averaged potential

tween two segments when the average electrostatic potential converges to the values of their infinite materials, using the equation

$$E_{offset} = \left[E_{v/c} - \overline{\overline{V}}_{\mathrm{ZnO}}\right]_{\mathrm{ZnO}} - \left[E_{v/c} - \overline{\overline{V}}_{\mathrm{Cu_2O}}\right]_{\mathrm{Cu_2O}} + \Delta V, \quad (4)$$

where the first and second terms respectively represent the positions of the valence/conduction band ($E_{v/c}$) relative to those of the average electrostatic potentials for the ZnO and Cu_2O. The third term is the difference between the two macroscopic average potentials from ZnO to Cu_2O (Fig. 2).

2.3. Supercell

The first step in the calculation of the interface properties is the construction of the supercell. The supercell has to be periodic in all the three dimensions and must be large enough in order to describe both ZnO and Cu_2O bulk and interface regions. ZnO crystallizes in the wurtzite structure, which is classified as a hexagonal lattice belonging to the space group $P6_3mc$ [7]. ZnO crystals generally grow along the c-axis by alternating layers of Zn^{++} and O^{2-}. This atomic arrangement along the c-axis leads to a polar crystal along the hexagonal longitudinal c-axis. This polarity imposes a growth direction for Cu_2O.

Several experimental and theoretical studies [16, 18, 35, 36] have demonstrated that on the ZnO substrate, Cu_2O grows according to the hexagonal symmetry. Because Cu_2O has the cuprite structure under standard thermodynamic conditions, it is usually accepted that the growth occurs along the [111] direction of the cubic lattice. In this study, we consider the possibility of a Cu_2O growth of the CdI_2 type, which differs from the cubic one for the stacking of Cu and O planes. In the CdI_2 structure, each O plane is between two Cu planes, and therefore this arrangement gives rise to a stoichiometric superlattice. As already noticed in the introduction, Cu_2O transforms into a CdI_2-type phase under pressure, as it was shown both experimentally [39] and theoretically [11]. To simulate the ZnO/Cu_2O heterojunction, we have built the supercell formed by 8 layers shown in Fig. 3. The structures of ZnO, Cu_2O, and the superlattice ZnO/Cu_2O have been fully relaxed. The resulting lattice parameters are reported in Table 1.

3. RESULTS AND DICSUSSION

The supercell method was employed in the study of the ZnO/Cu_2O heterojunction. The atomic arrangements in Cu_2O and ZnO(0001) suggest that it is energetically favorable for Cu_2O to grow on the ZnO(0001) substrate [40]. In the ZnO/Cu_2O heterojunction, the influences may be more obvious because of the large mismatch between cubic Cu_2O ($a = 4.27$ Å) and wurtzite ZnO ($a = 3.25$ Å and $c = 5.21$ Å) [15]. We found a possible way of lattice matching with a small lattice mismatch for Cu_2O thin films deposited on ZnO substrate (see Table 1).

In this study, we chose Cu_2O (CdI_2-type) and ZnO(0001). In this case, the Cu_2O lattice should be compressed and the Cu–O bond length decreased, which explains the choice of the high-pressure phase of Cu_2O. We use the lattice constants $a = 3.085$ Å and $c = 9.479$ Å for both materials; these values are the average of the optimization of the lattice parameters. The potential average $\overline{V}(z)$ and macroscopic average $\overline{\overline{V}}(z)$ profiles in the supercell containing a heterojunction are plotted in Fig. 2. This figure shows a sinusoidal shape that corresponds to the periodicity of the heterojunction. We observed a macroscopic average potential, shown by the dashed curve, flat over a wide area. This observation shows that the size of our supercell can give accurate results. The macroscopic average potential shows the discontinuity $\Delta V = 5.66$ eV at the interface (see Fig. 2).

In the regions far from the interface, the crystal should recover properties of the bulk. We find that

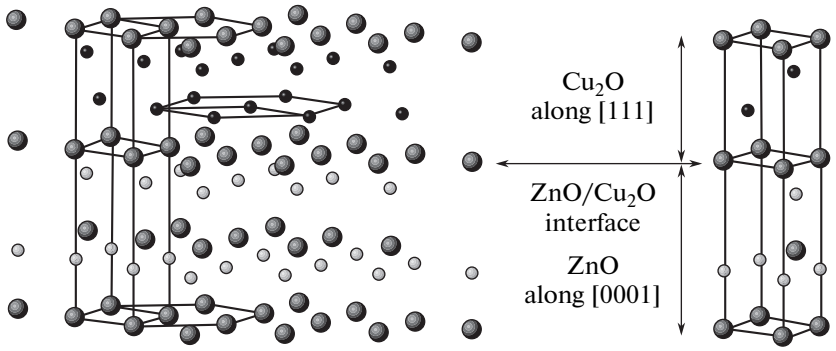

Fig. 3. The supercell model considered in this paper. The ZnO crystal grows along the c-axis and Cu_2O is in the hexagonal structure (CdI_2-type): large black balls, oxygen; small black balls, copper; gray balls, zinc

Table 1. Space group and lattice constant of ZnO, Cu_2O, and the supercell ZnO/Cu_2O

Compound	Structure	Space group	Lattice constants, Å		
ZnO	Wurtzite	$P6_3mc$ (186)	$a = 3.192$	$c = 5.190$	This work
			$a = 3.238$	$c = 5.232$	Other cal. [37]
			$a = 3.250$	$c = 5.207$	Exp. [38]
Cu_2O	Hexagonal	P-$3m1$ (164)	$a = 2.480$	$c = 3.900$	This work
			$a = 2.802$	$c = 4.393$	[18]
			$a = 2.900$	$c = 3.862$	Exp. [36]
ZnO/Cu_2O			$a = 3.085$	$c = 9.479$	This work

Table 2. Valence band offsets for the ZnO/Cu_2O system

Valence band offset, eV	Reference
1.51	This work
1.7	Exp. [14]
1.3–1.6	Others cal. [14]
2.2	Others cal. [12, 39]

the valence band maximum is -2.117 eV in ZnO and -3.627 eV in Cu_2O.

The application of Eq. (4) gives the value of the valence-band offsets. This value $\Delta E_v = 1.51$ eV (Table 2) includes varying theoretical and experimental results of the valence band alignment. The experimentally obtained ΔE_v is 1.7 eV, and the theoretical values obtained by the first-principle calculation are 1.3–1.6 eV. A large value $\Delta E_v = 2.2$ eV was found using electron affinity [39].

To calculate the conduction band alignment, we have used the experimental values of the gap energy because theoretical values, in the local density approximation, are underestimated and give incorrect values. In this work, we have used E_g respectively equal to 3.37 eV and 2.1 eV for ZnO and Cu_2O [14, 16]. The conduction band offset ΔE_c is evaluated as 0.24 eV. Our value is in good agreement with other values, although other works have already chosen simplified structures while we choose a more realistic one [14]. Ichimura and Song [14] have built a supercell by two oxides, ZnO and Cu_2O, in the same zincblende structure. This choice is a first step to study this system with less complication in the calculation and in building the supercell; however, this model is not too realistic.

The agreement between theoretical and experimental results shows that the DFT coupled with the theory of Van de Walle and Martin is reliable to determine the energy offset. We have investigated the electronic properties by calculating the density of states (DOS). The total DOSs are shown in Fig. 4. The difference between the DOS in the cuprous and CdI_2 structures is

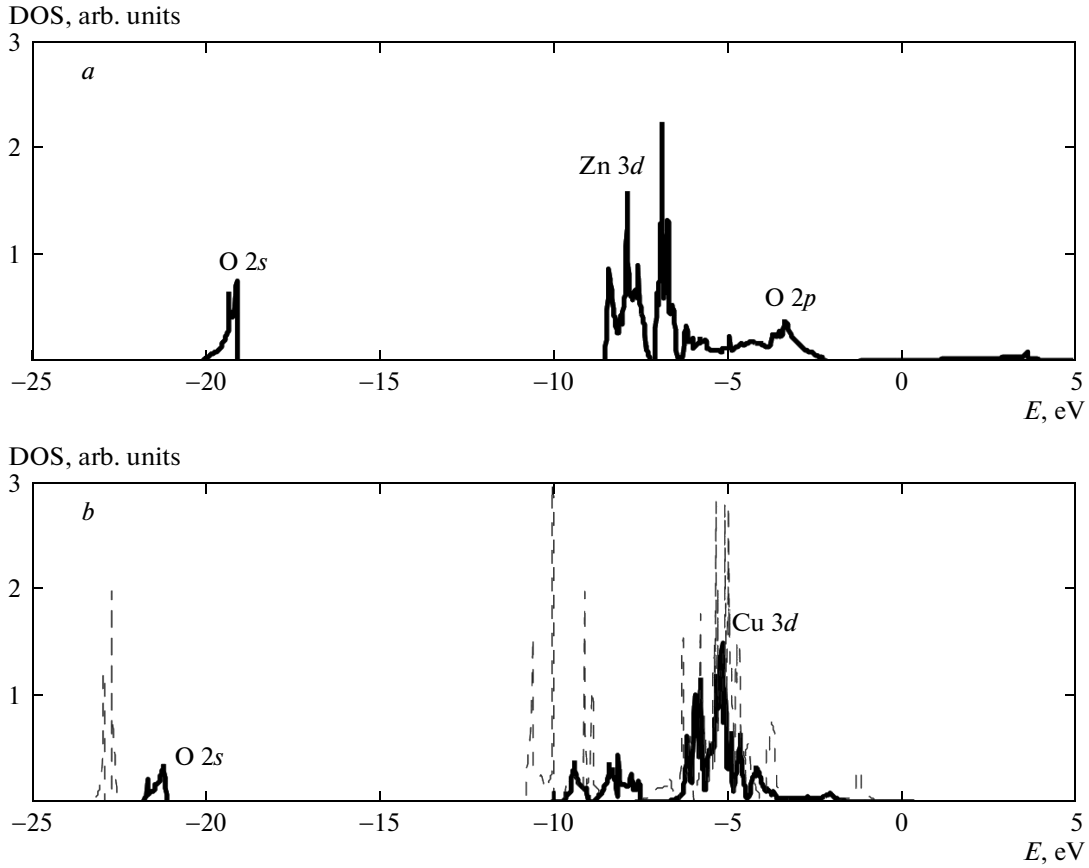

Fig. 4. Density of states of bulk (*a*) ZnO and (*b*) Cu_2O (the solid line is for Cu_2O type CdI_2 and the dashed line corresponds to the Cu_2O cuprous)

clear especially for the O $2s$ orbital. The valence band top of Cu_2O receives the main contribution from the Cu $3d$ orbital, and that of ZnO, from O $2p$. We show in Fig. 4 that the atomic energy level of Cu $3d$ is higher than that of O $2p$ by about 3 eV. This is considered as the principal reason why the valence band maximum of Cu_2O is higher than that of ZnO in the ZnO/Cu_2O system.

4. CONCLUSION

In this study, we have investigated the structural and electronic properties of the ZnO/Cu_2O heterojunction. The band alignment analysis is performed using the average potential and density of states. We presented the method of Van de Walle and Martin to calculate the energy offset. This approach fits well with the density functional theory. We began this work by constructing a supercell containing a junction formed by ZnO/Cu_2O. We selected the CdI_2 structure of copper oxide deposited on zinc oxide of wurtzite structure. Our calculations of the band offset gave a value that corresponds to the experimental and theoretical values already published in the literature. This study is very promising in understanding the transport properties and atomic formation mechanism of heterojunctions. It opens up the way to more extensive studies with this accurate theoretical method.

One of the authors, M. Zemzemi, wishes to thank Professor Pietro Cortona for the helpful discussions.

REFERENCES

1. B. Parida, S. Iniyan, and R. Goic, Renew. Sustain. Energ. Rev. **15**, 1625 (2011).

2. O. Shevaleevskiy, Pure Appl. Chem. **80**, 2079 (2008).

3. A. Zunger, S. Wagner, and P. Petroff, J. Electron. Mater. **22**, 3 (1993).

4. T. Surek, J. Cryst. Growth **275**, 292 (2005).

5. *Zinc Oxide — A Material for Micro- and Optoelectronic Applications*, ed. by N. H. Nickel and E. Terukov, Springer (2005).

6. D. C. Look, Mater. Sci. Eng. B **80**, 383 (2001).

7. Ü. Özgür, Y. I. Alivov, C. Liu et al., J. Appl. Phys. **98**, 04130 (2005).

8. B. P. Rai, Sol. Cells **25**, 265 (1988).

9. R. N. Briskman, Sol. Energy Mater. Sol. Cells **27**, 361 (1992).

10. J. Herion, E. A. Niekisch, and G. Scharl, Sol. Energy Mater. **4**, 101 (1980).

11. T. Minami, Y. Nishi, T. Miyata, and J. Nomoto, Appl. Phys. Express **4**, 062301 (2011).

12. B. Kramm, A. Laufer, D. Reppin et al., Appl. Phys. Lett. **100**, 094102 (2012).

13. S. S. Jeong, A. Mittiga, E. Salza et al., Electrochim. Acta **53**, 2226 (2008).

14. M. Ichimura and Y. Song, Jpn. J. Appl. Phys. **50**, 051002 (2011).

15. K. Akimoto, S. Ishizuka, M. Yanagita et al., Sol. Energ. **80**, 715 (2000).

16. K. Ozawa, Y. Oba, and K. Adamoto, Surf. Sci. **603**, 2163 (2009).

17. D. Manchon, V. V. Sinitsyn, V. P. Dmitriev et al., J. Phys.: Condens. Matter **15**, 7227 (2003).

18. P. Cortona and M. Mebarki, J. Phys.: Condens. Matter **23**, 045502 (2011).

19. M. Zemzemi, N. Elghoul, K. Khirouni, and S. Alaya, Zh. Eksp. Teor. Fiz. **145**, 272 (2013).

20. J. Tersoff, Phys. Rev. B **30**, 4874 (1984).

21. M. Cordona and N. E. Christensen, Phys. Rev. B **35**, 6182 (1987).

22. M. S. Hybertsen, Phys. Rev. Lett. **64**, 555 (1990).

23. C. G. Van de Walle and R. M. Martin, Phys. Rev. B **34**, 5621 (1986).

24. L. M. Wong, S. Y. Chiam, J. Q. Huang et al., J. Appl. Phys. **108**, 033702 (2010).

25. P. Hohenberg and W. Kohn, Phys. Rev. **136**, 864 (1964).

26. W. Kohn and L. J. Sham, Phys. Rev. **140**, 1133 (1965).

27. X. Gonze, J.-M. Beuken, R. Caracas et al., Comput. Mater. Sci. **25**, 478 (2002); http://www.abinit.org.

28. X. Gonze, B. Amadon, P.-M. Anglade et al., Comput. Phys. Comm. **180**, 2582 (2009).

29. N. Troullier and J. L. Martins, Phys. Rev. B **43**, 1993 (1991).

30. M. Fuchs and M. Scheffler, Comput. Phys. Comm. **119**, 67 (1999).

31. J. P. Perdew and Y. Wang, Phys. Rev. B **45**, 13244 (1992).

32. D. M. Ceperley and B. J. Alder, Phys. Rev. Lett. **45**, 566 (1980).

33. H. J. Monkhorst and J. D. Pack, Phys. Rev. B **13**, 5188 (1976).

34. S. H. Jeong and E. S. Aydil, J. Cryst. Growth **311**, 4188 (2009).

35. B. M. Fariza, J. Sasano, T. Shinagawa et al., Thin Solid Films **520**, 2261 (2012).

36. A. Werner and H. D. Hochheimer, Phys. Rev. B **25**, 5929 (1982).

37. F. Decremps, F. Datchi, A. M. Saitta, and A. Polian, Phys. Rev. B **68**, 104101 (2003).

38. S. Desgreniers, Phys. Rev. B **58**, 14102 (1998).

39. D. K. Zhang, Y. C. Liu, Y. L. Liu, and H. Yang, Physica B **351**, 178 (2004).

40. M. Yang, L. Zhu, Y. Li et al., J. Alloys Comp. **578**, 143 (2013).